

Superconductivity and correlated phases in non-twisted bilayer and trilayer graphene

Pierre A. Pantaleón,^{*} Alejandro Jimeno-Pozo, and Héctor Sainz-Cruz
Imdea Nanoscience, Faraday 9, 28049 Madrid, Spain

Võ Tiến Phong
Department of Physics and Astronomy, University of Pennsylvania, Philadelphia PA 19104, USA

Tommaso Cea
*Department of Physical and Chemical Sciences,
 University of L'Aquila, via Vetoio, Coppito, 67100 L'Aquila, Italy*

Francisco Guinea[†]
*Imdea Nanoscience, Faraday 9, 28049 Madrid, Spain and
 Donostia International Physics Center, Paseo Manuel de Lardizabal 4, 20018 San Sebastian, Spain*
 (Dated: May 29, 2023)

The discovery of a very rich phase diagram in twisted bilayer graphene [1, 2] renewed the interest into the properties of other systems based on graphene. An unexpected finding has been the observation of superconductivity in non-twisted graphene bilayers and trilayers [3–5]. In this perspective, we give an overview of the search for uncommon phases in non-twisted graphene systems. We first describe results related to the topic before the aforementioned experiments [3–5] were published. Then, we address the new experimental findings which have triggered the recent interest in the problem. Lastly, we analyze the already numerous theory works studying the underlying physical processes [6].

I. UNUSUAL PHASES IN NON-TWISTED GRAPHENE STACKS. EARLY RESULTS.

Graphite is considered a semimetal, with a highly complex Fermi surface, and a low density of states at the Fermi level. To a first approximation, graphite can be seen as a stack of two dimensional graphene layers. The low energy electronic properties of each graphene layer are well described by the two dimensional Dirac equation [7, 8]. This model shows that the density of states at the Fermi level vanishes, suggesting that electron interactions do not play a major role.

The isolation, and posterior detailed study [9, 10], of individual graphene layers lead to a search for effects of electronic interactions in single layer graphene, and also in bilayer graphene and in graphene multilayers. One of the most striking effects of the electronic interactions in single layer graphene is the renormalization of the Fermi velocity which characterizes the Dirac cones [11, 12], similarly to the renormalization processes in Quantum Electrodynamics. The degeneracy between Landau levels of monolayer graphene is also broken by interactions [13, 14].

The generalization of the Dirac equation to graphene (Bernal) bilayers [15, 16] replaces the two touching Dirac points by two touching parabolic bands. This structure leads to a logarithmically divergent susceptibility [17]. In the renormalization group language, this result implies that the screened Coulomb interaction is a marginally relevant perturbation, which leads to a variety of instabilities [18–21], including superconductivity. Superconductivity can also arise at high electron dopings, when the Fermi energy is close to a van Hove instability [22, 23]. Other graphene multilayers show interesting electronic bands, see, for instance [24]. In particular, an infinite rhombohedral stack is a Dirac semimetal [25], which implies that flat two-dimensional bands exist at the top and bottom surfaces, which can lead to correlated states [26]. Localized states at surfaces are likely in finite rhombohedral stacks [27, 28]. Finally, infinite graphene stacks can show stacking disorder (defected graphite), and, at the position of the defects, quasi-two-dimensional behavior may emerge [29–33]. Superconductivity in rhombohedral graphite has been predicted theoretically [34–36].

On the experimental side, superconductivity was observed in the so called graphite intercalation compounds, made up of metallic and graphene layers [37–39], with critical temperatures up to $\sim 10 - 12$ K. Superconductivity at higher temperatures, ~ 30 K has been found in fullerenes, C_{60} , crystals doped with alkaline ions [40–44]. In both cases, the

^{*}Electronic address: ppantaleon@uabc.edu.mx

[†]Electronic address: paco.guinea@gmail.com

amount of charge transferred to the carbon systems is considerable, $\sim 0.1 - 1 e/\text{atom}$, much larger than typical electrostatic dopings achieved in few layer graphene stacks. The electronic bands of graphite intercalation compounds and alkali doped fullerenes are quite different from the bands of graphene and graphite, and there is no clear evidence for unconventional superconductivity, although the effect of electron-electron interactions has been invoked in the doped fullerenes [45–51].

In addition, some early results suggested the existence of correlated phases in Bernal bilayers [52–57] and also in *ABC* trilayers [58–60]. Some observations of electronic gaps in transport measurements can be due to domain walls in the bilayers [61]. Unusual phases have also been reported in other graphene trilayers [58, 62, 63], and also in thicker multilayers [64–66].

Finally, it is worth remarking that a number of works report phenomena compatible with superconductivity in bulk graphite [67–74]. It is unclear the role that two dimensional electron gases trapped at stacking defects can play in these observations [29–33, 70, 73].

II. SUPERCONDUCTIVITY IN BERNAL BILAYER AND RHOMBOHEDRAL TRILAYER GRAPHENE

A. Bilayer graphene

Superconductivity in Bernal bilayer graphene was discovered by Zhou *et al.* [3]. This material is the most common allotrope of graphene because its stacking is the structural ground state of two graphene layers [75, 76]. The experiments in Ref. [3] consist of inverse compressibility and magneto-resistance measurements on bilayer graphene encapsulated in non-aligned hBN and graphite gates. Upon applying a displacement field perpendicular to the layers, a gap opens at charge neutrality, while the bands develop a ‘Mexican hat’ dispersion, leading to van Hove singularities that promote strong correlations. In this setup, Ref. [3] shows a map of the inverse compressibility $\kappa = \partial\mu/\partial n_e$, where μ is the chemical potential, as a function of hole doping n_e and displacement field D . The map reveals a series of dips in κ , which delineate different regions in the phase space defined by n_e and D , see Fig. 1(a). Furthermore, measuring the magneto-resistance yields the frequency of quantum oscillations normalized to n_e , f_ν , which is the fraction of the Fermi surface enclosed by a cyclotron orbit. The results show that f_ν , and hence the number of pockets in the Fermi surface, is different in each region. Together, these phenomena indicate a cascade of transitions between flavour-symmetry-breaking metallic phases, which resemble those observe in twisted graphene stacks [77–79] and RTG [80], as well as Lifshitz transitions which change the topology of the Fermi surface. Subsequent experiments have studied in great detail the correlated phases of bilayer graphene [81, 82]. In particular, on top of the flavour polarized metals, Ref. [82] reports the observation of several new phases, such as correlated metals with linear-in-temperature resistivity, a Wigner crystal, and a novel Wigner-Hall crystal, an electron crystal which has a quantized Hall conductance.

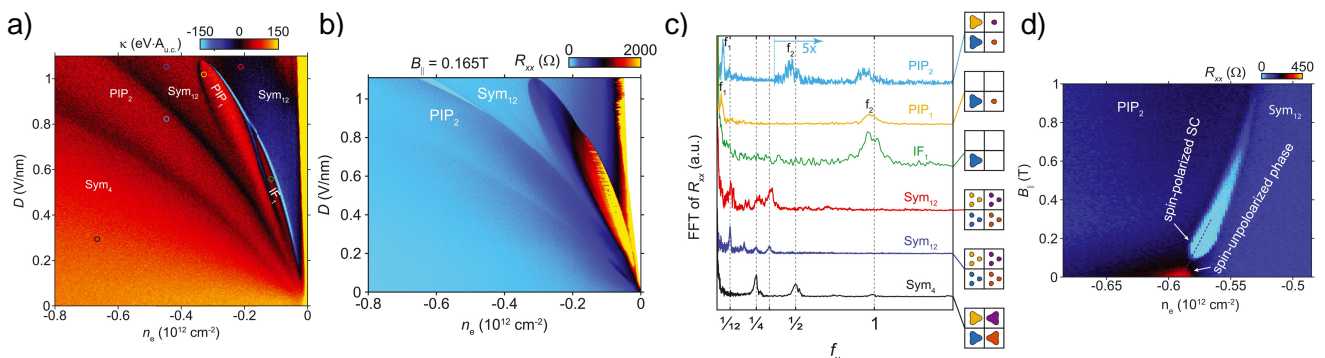


Figure 1: Superconductivity in bilayer graphene. (a) Inverse compressibility without magnetic field, as a function of electron doping n_e and displacement field D . (b) Longitudinal resistivity (R_{xx}) at $T = 10$ mK and $B_{||} = 165$ mT, showing a superconducting sleeve in bright cyan. (c) Fast Fourier transform of the magneto-resistance versus frequency normalized to n_e , measured at circled points in (a). The insets show the inferred Fermi surfaces for each phase. (d) R_{xx} versus $B_{||}$ and n_e at $D = 1.02$ V/nm. Figures extracted from Ref. [3].

Upon applying an in-plane magnetic field, a superconducting sleeve appears near the boundary between two of these phases, as shown in Fig. 1(b), for dopings near where a van Hove singularity is expected. One of these phases,

dubbed ‘Sym₁₂’, appears to have twelve Fermi pockets (four flavours with three pockets each due to trigonal warping effects, see Fig. 5(f)) and the other, ‘PIP₂’, a symmetry-broken phase with two large and two small pockets, one per flavour, which may be nematic. Superconductivity manifests as vanishing resistivity, and a Fraunhofer pattern in the presence of a magnetic field, conclusive evidence of phase coherence. The critical temperature, deduced from non-linear transport and Berezinskii-Kosterlitz-Thouless theory, is $T_c \approx 26$ mK. At this temperature, a magnetic field of 40 mT would break the pairs of a conventional spin-singlet superconductor, since the Zeeman effect would overcome the superconducting gap. Superconductivity in bilayer graphene survives at fields over ten times larger than this Pauli limit, of $B \gtrsim 500$ mT, which is strong evidence of spin-triplet pairing.

The emergence of superconductivity is better understood by comparing transport experiments at zero and finite magnetic field, throughout the region of phase-space that becomes superconducting. At zero magnetic field, the sleeve between PIP₂ and Sym₁₂ is a state distinct from both, with higher resistance, and, most likely, insulating, see Fig. 1(d). Its resistance has non-linear behaviour and drops abruptly at a threshold in the applied current. Turning on and increasing a magnetic field (in- or out-of-plane) reduces this threshold until it vanishes, giving rise to superconductivity. This suggests that the resistive state is spin-unpolarized and that the superconducting state emerges from it when the magnetic field polarizes the spin.

A relevant measure of the level of disorder in the material is the ratio between the superconducting coherence length, estimated to be $\xi \approx 250$ nm and the electronic mean free path, of $l_M \approx 5$ μ m, comparable to the dimensions of the device. The ratio is $d = \xi/l_M < 0.05$, which implies an ultra-clean regime of superconductivity, in which pair-breaking effects due to non-magnetic impurities are weak, and which is therefore compatible with the unconventional spin-triplet pairing inferred from the rest of the data. A similar ratio is estimated in the experiments described next.

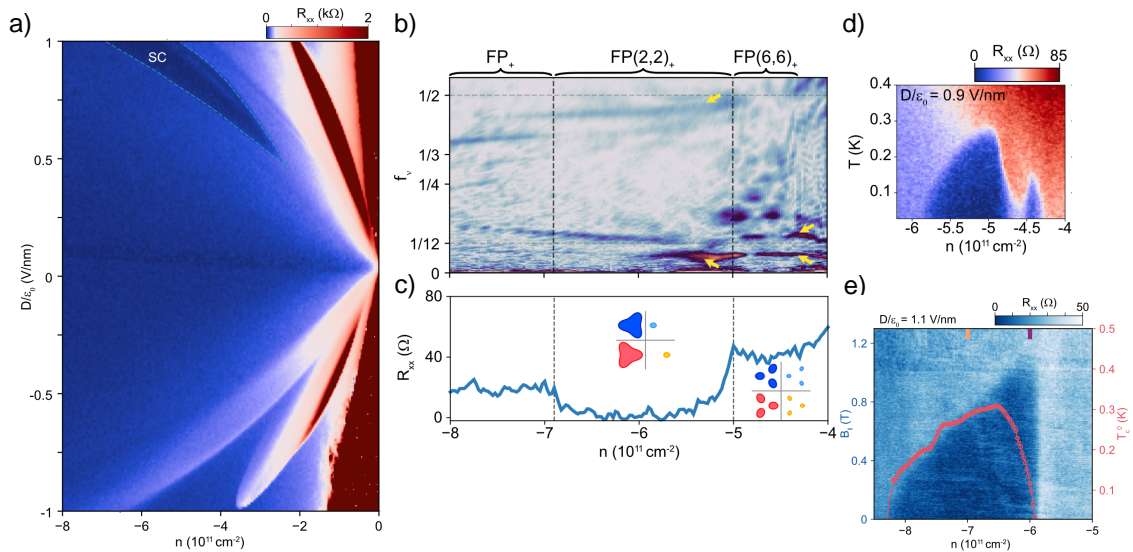


Figure 2: Superconductivity in bilayer with WSe₂. (a) R_{xx} versus hole doping and displacement field, at zero magnetic field, showing a superconducting sleeve in dark blue. (b) Fast Fourier transform of the magneto-resistance versus n_e . (c) Cut of the resistivity at $D = 1$ V/nm, insets show the Fermi surfaces inferred from (b). (d) R_{xx} as a function of doping and temperature for $D = 0.9$ V/nm. (e) R_{xx} versus doping and in plane magnetic field, at $D = 1.1$ V/nm. Red circles indicate the zero-field T_c . Figures extracted from Ref. [5].

The second set of ground-breaking experiments on bilayer graphene have been done by Zhang *et al.* [5]. The main idea was to stabilize superconductivity by placing tungsten diselenide (WSe₂) on top of the bilayer, a strategy that has already proved fruitful in twisted bilayer graphene, yielding superconductivity at record low twist angles [83]. For bilayer graphene, Ref. [5] reveals that the interplay with WSe₂ leads to a significant, global enhancement of superconductivity: it appears even in the absence of a magnetic field, its critical temperature increases by an order of magnitude, to $T_c \approx 260$ mK and the filling range of the superconducting sleeve is similarly extended, compare Fig. 2(a) to Fig. 1(a). There is compelling evidence that these effects are due to Ising spin-orbit coupling (SOC) induced by WSe₂. Note that in the absence of WSe₂ the SOC in bilayer graphene is negligible [84].

A key aspect of Fig. 2(a) is the asymmetry with respect to the D field direction. In particular, superconductivity appears just at positive D . Theory predicts that Ising SOC only couples to the top layer, which is next to WSe₂ [85, 86]. For hole doping, a positive D field pushes the wavefunction towards WSe₂, letting the carriers benefit from Ising SOC. For similar values of n_e , the phase at negative D fields is a resistive state that disappears upon applying magnetic

fields, which is most likely the same phase from which superconductivity emerges in Ref. [3]. It appears that this is also the phase that here, at positive D field, competes with superconductivity, cutting through the superconducting region and splitting it in two, see Fig. 2(d). A resistive state, flanked by superconducting domes, is reminiscent of the situation observed in e.g. twisted bilayer graphene [2]. These observations support the idea that Ising SOC contributes to superconductivity in the system.

Quantum oscillations confirm that the phase diagram observed in [5] at negative D field is almost identical to the one observed in bilayer graphene in [3], which shows a transition between the PIP_2 and Sym_{12} phases. In contrast, for positive D field, the data suggests that, due to band splitting induced by Ising SOC, the phase adjacent to PIP_2 has six large and six small Fermi pockets, so it is similar to PIP_2 but in the trigonal warping regime, see Fig. 2(b) and (c). Another difference is that superconductivity emerges from PIP_2 after Ising SOC presumably selects a symmetry-broken state that enables pairing, while in bilayer graphene encapsulated in hBN the parent state seems to be another one with higher resistance, see Fig. 1(d).

The critical magnetic field differs starkly on both sides of the superconducting dome, as shown in Fig. 2(e). The low n_e side violates the Pauli limit by a factor of six, while the high n_e barely does, perhaps hinting at a nuanced evolution of the Fermi surface with doping within the dome. A possibility is that the system develops Ising superconductivity, which promotes Cooper pairs of type $|K^+, \uparrow; K^-, \downarrow\rangle$, locking the spin and valley degrees of freedom and making the state very resilient to in-plane magnetic fields. However, as pointed in Ref. [5], the moderate critical fields observed may be more consistent with an Ising SOC-induced inter-valley coherent phase.

B. Trilayer graphene

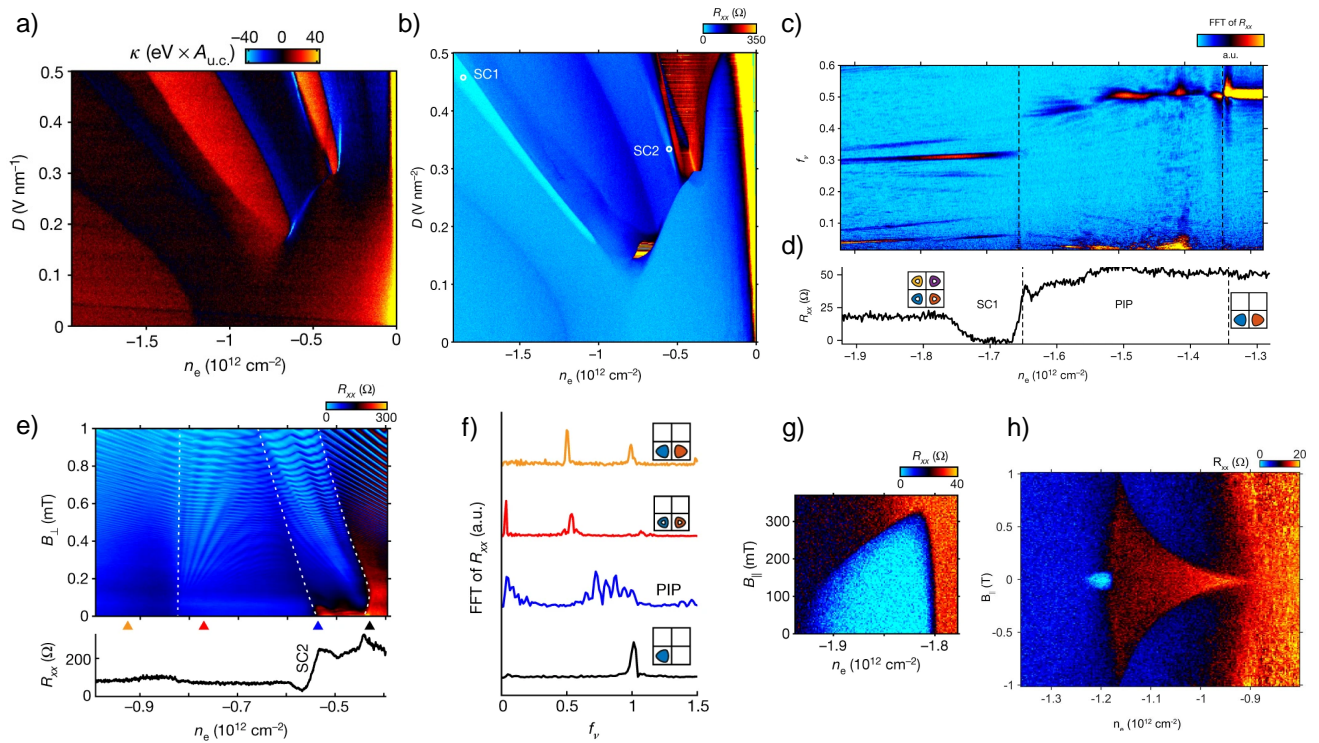


Figure 3: Superconductivity in RTG. (a) Inverse compressibility as a function of n_e and D . (b) R_{xx} versus n_e and D , showing two superconducting sleeves SC1 and SC2 in bright cyan. (c) Fast Fourier transform of R_{xx} as a function of n_e near SC1 and frequency f_ν . (d) R_{xx} versus n_e near SC1, at zero magnetic field. (e) Magneto-resistance versus n_e near SC2 (top) and R_{xx} versus n_e near SC2, at zero magnetic field (bottom). (f) Fast Fourier transform of (e), along the coloured arrows. (g) R_{xx} as a function of n_e and temperature, for SC1. (h) R_{xx} versus n_e and in-plane magnetic field, at the partially flavour polarized phase adjacent to SC1. Figures extracted from Ref. [80] and Ref. [4].

The experiments by Zhou *et al.* [4, 80] in rhombohedral trilayer graphene (RTG) reported unambiguous observations of correlated behaviour [80] and superconductivity [4] in a crystalline graphene system. Rhombohedral ABC stacking

is a metastable three layer allotrope of graphene, with Bernal *ABA* being the ground state, although recent results suggest *ABC* may be stable [87]. RTG is similar to BBG in that a perpendicular displacement field opens a gap and flattens the low-energy bands, setting the stage for strong correlations, although it is worth noting that RTG has flat bands even in the absence of a *D* field. In this material, inverse compressibility and magneto-resistance measurements also uncover a cascade of flavour-symmetry breaking transitions, see Fig. 3(a), including a spin-polarized half-metal phase and a spin- and valley-polarized quarter-metal. Ref. [80] uses a Stoner model, similar to the one in Ref. [77], to explain the cascade at positive filling. At negative fillings, shown in Fig. 3(a), the situation is more nuanced, due to the interplay between flavour symmetry breaking and Lifshitz transitions, which gives rise to several partially flavour polarized phases. Superconductivity has been found in two regions, SC1 and SC2, of the phase space defined by n_e and *D*, as shown in Fig. 3(b). On top of vanishing resistivity, non-linear transport in the presence of a magnetic field yields Fraunhofer patterns, definitive evidence of superconductivity. The estimated critical temperatures are $T_{c1} = 106$ mK for SC1 and $T_{c2} = 50$ mK for SC2. Like in BBG, the superconducting sleeves in RTG appear close to flavour-symmetry-breaking transitions.

Quantum oscillations data near the SC1 superconducting sleeve, shown in Fig. 3(c), reveals that it arises from a symmetric state, Sym_4 , in which each flavour has an annular Fermi surface, and which is adjacent to a phase with a complex Fermi surface, spin-unpolarized and partially valley-polarized, probably with large and small Fermi pockets, like PIP_2 in BBG. On the other hand, SC2 emerges at the boundary between a spin-polarized, valley-unpolarized half-metal and a partially-flavour polarized state, which also appears to have large and small Fermi pockets, see Fig. 3(f). Further differentiating these two superconducting regions, SC1 shows only a small Pauli limit violation, and its T_c dependence on *B* is compatible with conventional spin-singlet pairing. Still, it is worth noting that the critical magnetic field is very asymmetric with respect to n_e , like in BBG-WSe₂, compare Fig. 3(g) and Fig. 2(e). In stark contrast, SC2 violates the Pauli limit by an order of magnitude. Moreover, spin-singlet pairing for SC2 is precluded by the fact that its parent state is spin-polarized, so the two spin orientations are separated by the exchange interaction energy ($\sim 1 - 10$ meV), over two orders of magnitude greater than the superconducting gap. Therefore, there is strong evidence that SC2 is a spin-triplet superconductor. Just like in BBG, an estimate of the level of disorder gives $d \sim 0.05$, so the system is clean enough to support unconventional spin-triplet pairings.

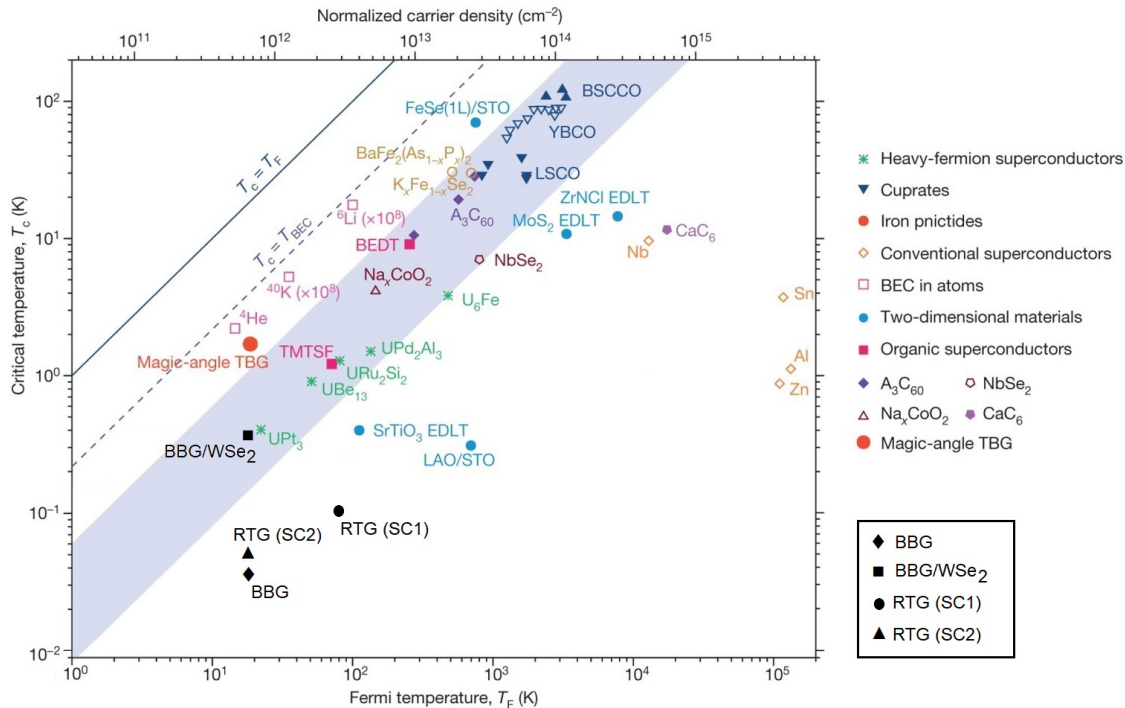


Figure 4: Logarithmic plot of critical temperature T_c versus Fermi temperature T_F for various superconductors. Black shapes correspond to non twisted graphene systems. Adapted from Ref. [2]

C. Comparison to twisted stacks

It is illustrative to compare the superconductivity and correlated phases observed so far in twisted and non-twisted stacks. Some of the similar features shared by both types of stacks are that (i) superconductivity occurs at very low carrier densities. The density in twisted bilayer graphene is determined by the number of electrons which can be accommodated into the central bands, while in non-twisted systems the density is fixed by the states available in the flat regions of the low energy bands. In both cases these estimates give $n_e \sim 10^{12} \text{ cm}^{-2}$. Knowledge of n_e allows for the classification of interactions according to their strength, and reveals that the long range Coulomb interaction, $V_C \approx e^2 k_F \propto e^2 \sqrt{n_e}$, is larger than the bandwidth and it is parametrically larger than other interactions [88], which scale as n_e . Also, superconductivity: (ii) violates the Pauli limit, indicating that the pairing is, at least in part, spin-triplet; (iii) is adjacent to correlated insulators [2, 3, 5, 89–93] and (iv) is modified when the graphene stack is in proximity of a WSe₂ monolayer [5, 83]. In addition, there are (v) cascades of flavour-symmetry breaking transitions [3–5, 77, 78, 80–82]; (vi) Quantum Anomalous Hall phases [80, 82, 94] and (vii) strange metals with linear-in-temperature resistivity [82, 95].

The most notable differences include: (i) $T_c \sim 1 \text{ K}$ in twisted stacks, and $T_c \sim 10 - 100 \text{ mK}$ in non-twisted stacks. Since the densities are similar, this means that twisted stacks are in a regime of stronger coupling, see Fig. 4. (ii) Superconductivity in non-twisted stacks appears only when applying a displacement field. (iii) The relevant bands are isolated from the rest of the spectrum only in twisted stacks with an even number of layers. (iv) Angle disorder, strain and lattice relaxation have a serious impact on twisted stacks. (v) In proximity of a WSe₂ monolayer, T_c is enhanced in BBG, while in twisted bilayer graphene superconductivity is stabilized at a lower angle, but T_c does not increase. (vi) Some phenomena have only been observed in twisted stacks, e.g. Chern insulators [96–102], nematicity [103], Pomeranchuk effect [104, 105] or re-entrant superconductivity with a magnetic field [91], while others like the Wigner and Wigner-Hall crystals have only been seen in BBG [82].

III. THEORETICAL MODELS

A. Non-interacting band structures

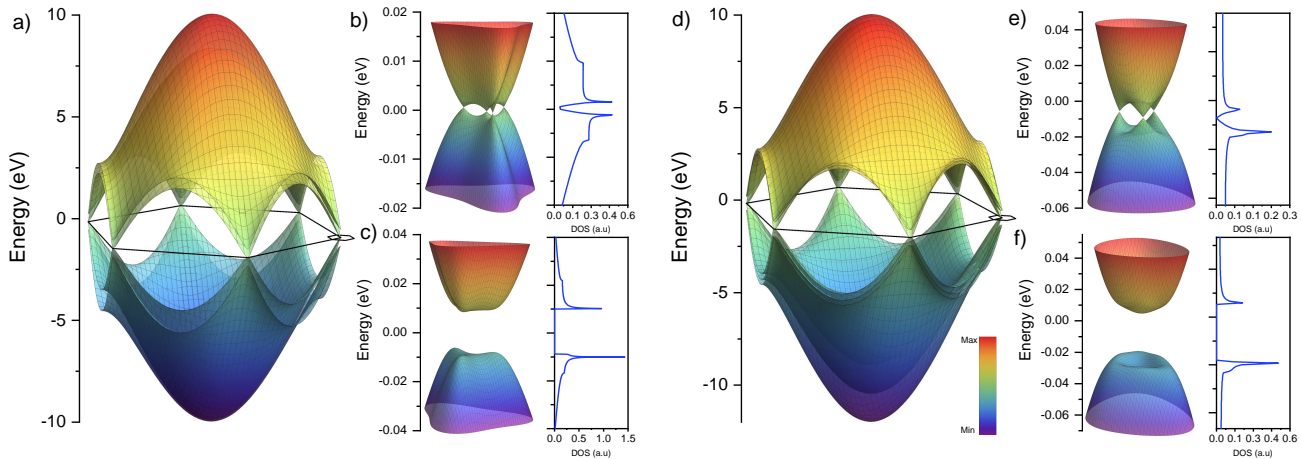


Figure 5: Band structure in the full Brillouin zone for: a) Bernal bilayer graphene and d) rhombohedral trilayer graphene. The large hexagon near zero energy is the corresponding Brillouin zone. The small hexagon is the Dirac point where the low energies of the corresponding system are calculated for b) and e) zero and c) and f) 20 meV perpendicular displacement field. At the side of the low energy bands is the corresponding density of states. The model and parameters for the figures are given in Ref. [16]

Both RTG and BBG become superconductors at very low electronic densities $n_e \sim 10^{12} \text{ cm}^{-2}$ when an electric field is applied perpendicular to the graphene system. From the theoretical point of view is universally accepted that the band flattening resulting from the displacement field and the consequent van Hove singularities enhance the role of interactions. The study of the electronic properties is usually performed with low energy continuum models with the exception of Ref. [106] which studied the superconductivity using a tight binding model. The non-interacting tight binding band structure [16], low energy regions and density of states of RTG and BBG is shown in Fig. 5. In BBG there are two vertically aligned graphene layers so that atoms belonging to the sublattice *A* of layer 1 lie over the atoms

in the sublattice B of layer 2. Similarly to monolayer graphene, BBG is a semi-metal in which the low energy bands touch at the Dirac points, but with parabolic instead of linear dispersion [15, 107]. This band touching makes the charge susceptibility and other susceptibilities diverge [17], which leads to symmetry-broken phases [18–21, 108–110]. As a perpendicular electric field is applied, inversion symmetry is broken, and the Dirac points connecting the bands become gapped. As a result, the local band dispersion can be nearly quenched. As shown in Fig. 5(b) and (c), the low energy bilayer bands acquire a ‘Mexican hat’ profile [111].

Rhombohedral trilayer graphene is a semi-metal with an approximate cubic band degeneracy at the zone corners [7, 24, 26–28, 30, 34, 35, 37, 56, 112] where optimal parameters have been reported in the literature [24, 27, 63, 113]. Close to the Dirac points, the cubic degeneracy resulting from diagonalizing the Hamiltonian splits into three Dirac cones, creating a trigonally-warped Fermi surface, shown in Fig. 5(e). A perpendicular electric field breaks inversion symmetry, and these Dirac points acquire a finite mass, Fig. 5(f). As a result, the local band dispersion is flattened, generating a van Hove singularity that favors the emergence of correlated electronic phases.

Table I: Overview of theories of superconductivity in bilayer and trilayer graphene systems, according to their proposed pairing mechanism, estimated critical temperature T_c and symmetry of the superconducting order parameter (OP).

System	Pairing mechanism	T_c (mK)	OP symmetry	OP sign change
BBG	Phonons [114, 115]	1000 - 2000 (no $e-e$ interactions), 20-500 (with $e-e$ interactions)	Spin-triplet [116], valley singlet (f -wave), intra-valley: singly degenerate, A .	Most likely, no
	Short range, momentum independent interactions, proximity to broken symmetry phases [117]	—	Spin-triplet (f -wave).	—
	Quantum critical modes [118]	35	Spin-triplet, valley-singlet s -wave or spin-triplet, valley-triplet (f -wave).	—
	Screened long-range Coulomb [119]	10	Spin-triplet, valley-singlet (f -wave), intra-valley: singly degenerate, A , or doubly degenerate, E .	Yes
	Short-range Coulomb [120]	20	Spin-triplet, valley-singlet (f -wave).	Most likely, no
BBG-WSe ₂	Phonons + substrate tunneling [121]	—	Mixture of spin-singlet, valley-triplet (s -wave) and spin-triplet, valley-singlet (f -wave)	—
	Screened long-range Coulomb [119]	12-40	Ising superconductor, intra-valley: singly, A , or doubly degenerate, E .	Yes
RTG	Phonons [122]	500 - 1600	Spin-singlet, valley-triplet (unpolarized normal state), spin-triplet, valley-singlet (polarized normal state)	Most likely, no
	Short range, momentum independent interactions, proximity to broken symmetry phases [123]	—	Spin-triplet (f -wave).	—

Continued on next page

Table I: Overview of theories of superconductivity in bilayer and trilayer graphene systems, according to their proposed pairing mechanism, estimated critical temperature T_c and symmetry of the superconducting order parameter (OP). (Continued)

	Flavour fluctuations [124]	—	Spin-singlet, valley-triplet, singly degenerate, A	Most likely, no
	Flavour fluctuations [125]	—	Dependent on details of interactions	Dependent on details of interactions
	Intervalley fluctuations [126]	—	Spin-singlet, valley-triplet	—
	Screened long-range Coulomb [119, 127]	65-140	Spin-triplet, valley-singlet (f -wave), intra-valley: singly degenerate, A , or doubly degenerate, E .	Yes
	Screened long-range Coulomb [128]	0 - 2000, depending on dielectric constant	Two pockets in each valley, spin singlet, d -wave (doubly degenerate), or spin triplet, p -wave (doubly degenerate), depending on inter-pocket couplings	Most likely, yes
	Screened long-range Coulomb [129]	Depends on coupling constant, λ . T_c covers a broad range.	Depends on details of intervalley coupling.	Yes
	Few momentum independent interactions [130]	—	Spin triplet, valley-singlet or spin-singlet, valley-triplet, depending on sign of inter-valley Hund coupling	—
	Short-range Coulomb [131]	—	Spin-singlet, d -wave (at half filling only)	—
	Short-range Coulomb [120]	20-140	Spin-triplet, valley-singlet (f -wave).	Most likely, no
	Short-range Coulomb [132]	—	$d + id$.	—
RTG-WSe ₂	Screened long-range Coulomb [119]	65-70	Ising superconductor, intra-valley: singly degenerate, A , or doubly degenerate, E .	Yes

B. Superconducting mechanisms

It is worth first to describe some general features of the superconducting state. The symmetries of the hamiltonian constrain the possible superconducting order parameters. The existence of two valleys implies that the order parameter can be even or odd with respect to valley exchange. If we neglect spin-orbit coupling, the Pauli principle implies that a valley symmetric order parameter is a spin-singlet, while a valley antisymmetric order parameter is a spin-triplet. The lowest symmetry that the bilayer and trilayer in a perpendicular field has around the K and K' points is a C_3 rotation. This symmetry allows for two representations, a non degenerate one, A , and a doubly degenerate one, E . Spin-orbit coupling mixes valley and spin exchange. The simplest case where the spin-orbit coupling only affects the out of plane spin direction, s_z , leads to Ising superconductivity, where the spin and valley degrees of freedom are locked [133]. Finally, depending on the sign and relative strength of intra- and inter-valley interactions, the order parameter can show changes of sign and nodes at the Fermi surfaces, an example is shown in Fig. 6.

Using this analysis of the superconducting state, a classification of different theoretical models is given in Table I

for both Bernal bilayer and *ABC* trilayer. Three general pairing mechanisms have been considered: i) electron-phonon coupling [114, 115, 121, 122], ii) electronic fluctuations associated to the proximity of broken symmetry phases [117, 118, 123–126], and iii) direct repulsive electron-electron interactions, either the long range Coulomb potential [119, 127–130] or short range interactions [120, 131, 132]. These pairing mechanisms have been studied using a variety of formalisms: i) standard BCS calculations [114, 115, 121, 122], ii) diagrammatic methods inspired by the Kohn-Luttinger [134] formalism [119, 120, 126, 127], the renormalization group [128, 130], phenomenological electronic susceptibilities describing nearby broken symmetry phases [117, 118, 124, 126], or numerical Monte Carlo analyses [131]. Different approximations require the knowledge of different number of parameters.

The changes of sign of the order parameter at the Fermi surfaces determine the robustness of the superconducting phase against elastic scattering. When the order parameter has different signs in the two valleys, short range scattering is pair breaking. If the order parameter changes sign within the pockets in each valley, long range scattering is also pair breaking. It is worth mentioning that long range repulsive interactions can lead to a superconducting state because the screened interaction is less repulsive at $\mathbf{q} = 0$ than at finite values of \mathbf{q} , so that an order parameter with sign changes is allowed [135].

Finally, we compare the results of the theoretical proposals collected in Table I with the experimental findings in Refs. [3–5]. In BBG, which has a measured critical temperature of $T_c \approx 26$ mK, the theories in which pairing is due to purely electronic interactions [117–120] yield critical temperatures and superconducting dome widths of the same order of magnitude as the experiments, while in the theory where pairing is mediated by phonons [114, 115] the predicted critical temperatures and the width of the superconducting dome are larger than in experiments. Identical conclusions apply to RTG. When a monolayer of WSe₂ is placed on top of BBG, the critical temperature goes up by an order of magnitude, reaching $T_c \approx 260$ mK. In this setup, Ref. [121] shows that virtual tunnelling to the substrate can favour the attraction between two holes and boost the phonon-driven superconducting T_c , although an estimate of the enhancement is not given. Ref. [119] proposes a Kohn-Luttinger-like mechanism for superconductivity and shows that, due to reduced screening of the Coulomb interaction at intermediate momenta, Ising spin-orbit coupling enhances the superconducting T_c by a factor of 4 in BBG. The associated order parameter shows locking between the spin and valley degrees of freedom.

Most theories either predict, or are compatible with spin-triplet pairing, in agreement with the Pauli limit violations seen in experiments. Furthermore, some proposals based on the screened long-range Coulomb interaction [119, 127] predict the form of the superconducting order parameter, which shows intravalley nodes and sign changes, see Fig. 6. As mentioned above, these sign changes make superconductivity fragile against long-range disorder, and may explain why it has eluded discovery until now.

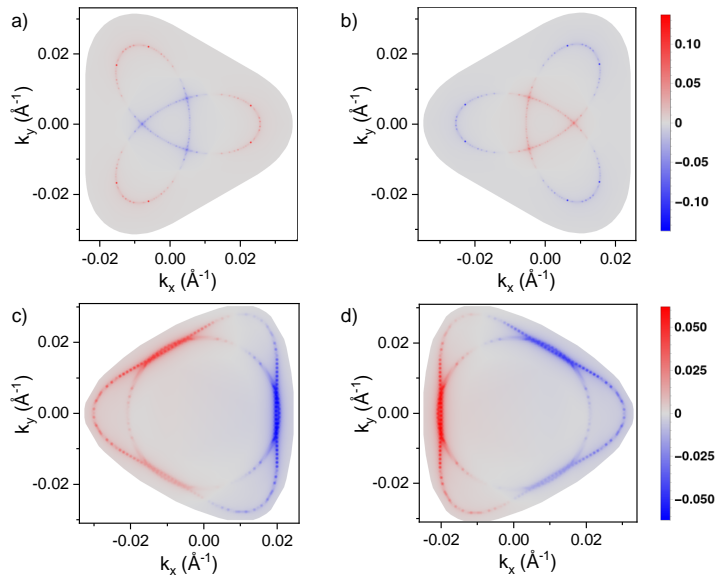


Figure 6: (a) Superconducting order parameter (OP) of BBG in valley K^+ , (b) in valley K^- , near the hole-doped van Hove singularity, with $T_c \approx 10$ mK. Within a single valley, the OP peaks along the edges of the Fermi surface and changes sign between the inner and outer edges. (c) OP of RTG in valley K^+ , (d) in valley K^- , near the hole-doped van Hove singularity and with $T_c \approx 65$ mK, showing intensity stripes along the edges of the Fermi surface. C_3 -symmetry is broken because the intravalley symmetry is E , degenerate. In both materials, the OP changes sign between valleys, which means that BBG and RTG are valley-singlet, spin-triplet superconductors. Data replotted from Ref. [119]

C. Other theoretical results.

The analyses described in the previous subsection give also information on the nature of the normal state, especially those ones which assume that superconductivity emerges from a broken symmetry phase. In addition, the role of the electron-electron interaction in the normal state of RTG has been studied in [136], where the effects of strong local interactions are described using Dynamical Mean Field Theory. Non superconducting broken symmetry phases in RTG are analyzed phenomenologically in [137]. The information that the optical conductivity gives on correlated phases in RTG has been studied in [138]. Superconductivity has also been predicted to exist in rhombohedral tetralayer graphene [115, 139].

IV. CONCLUSIONS

The crystalline nature of bilayer and trilayer graphene is a crucial advantage with respect to twisted systems, which suffer from twist angle disorder [140] and strains [141]. These issues place strict demands on the fabrication process and hinder experimental reproducibility [142]. In contrast, bilayer and trilayer graphene are mechanically stable, easy to fabricate, and have very low disorder and strain. Given the complexity of the phase diagrams to elucidate, bypassing the issue of disorder may prove decisive in the pursuit of a unified theory of superconductivity and strongly correlated phases in graphene based superconductors.

The observation of superconductivity and other non trivial phases in non-twisted graphene bilayers and trilayers suggests that other graphene based compounds, suitably modified, can also support correlated electronic phases. Non-twisted stacks, like the ones discussed here, probably can be tuned to show flat bands. Note that, on the other hand, not all twisted graphene stacks show superconductivity [143, 144].

Superconductivity has not been found yet in twisted transition metal dichalcogenides (TMD's), or in TMD heterobilayers, although there is ample evidence of other correlated phases [145].

Finally, it is worth considering whether the mechanism which triggers superconductivity is the same in twisted and non-twisted carbon compounds.

V. ACKNOWLEDGMENTS.

We are thankful to Andrey V. Chubukov, José A. Silva-Guillen, Elena Bascones and Gerardo Naumis for illuminating discussions. We acknowledge support from the Severo Ochoa programme for centres of excellence in R&D (Grant No. SEV-2016-0686, Ministerio de Ciencia e Innovación, Spain); from the European Commission, within the Graphene Flagship, Core 3, grant number 881603 and from grants NMAT2D (Comunidad de Madrid, Spain), SprQuMat (Ministerio de Ciencia e Innovación, Spain) and (MAD2D-CM)-MRR MATERIALES AVANZADOS-IMDEA-NC. V.T.P. acknowledges support from the Department of Energy under grant DE-FG02-84ER45118, the NSF Graduate Research Fellowships Program, and the P.D. Soros Fellowship for New Americans.

-
- ¹ Yuan Cao, Valla Fatemi, Ahmet Demir, Shiang Fang, Spencer L. Tomarken, Jason Y. Luo, Javier D. Sanchez-Yamagishi, Kenji Watanabe, Takashi Taniguchi, Efthimios Kaxiras, Ray C. Ashoori, and Pablo Jarillo-Herrero. Correlated insulator behaviour at half-filling in magic-angle graphene superlattices. *Nature*, 556(7699):80–84, apr 2018. ISSN 14764687. doi: <https://doi.org/10.1038/nature26154>. URL <https://doi.org/10.1038/nature26154>.
 - ² Yuan Cao, Valla Fatemi, Shiang Fang, Kenji Watanabe, Takashi Taniguchi, Efthimios Kaxiras, and Pablo Jarillo-Herrero. Unconventional superconductivity in magic-angle graphene superlattices. *Nature*, 556:43, 03 2018. URL <https://doi.org/10.1038/nature26160>.
 - ³ Haoxin Zhou, Ludwig Holleis, Yu Saito, Liam Cohen, William Huynh, Caitlin L. Patterson, Fangyuan Yang, Takashi Taniguchi, Kenji Watanabe, and Andrea F. Young. Isospin magnetism and spin-polarized superconductivity in Bernal bilayer graphene. *Science*, 375(6582):774–778, feb 2022. ISSN 10959203. doi: 10.1126/science.abm8386. URL <https://www.science.org/doi/10.1126/science.abm8386>.
 - ⁴ Haoxin Zhou, Tian Xie, Takashi Taniguchi, Kenji Watanabe, and Andrea F. Young. Superconductivity in rhombohedral trilayer graphene. *Nature*, 598(7881):434–438, oct 2021. ISSN 14764687. doi: 10.1038/s41586-021-03926-0.
 - ⁵ Yiran Zhang, Robert Polski, Alex Thomson, Etienne Lantagne-Hurtubise, Cyprian Lewandowski, Haoxin Zhou, Kenji Watanabe, Takashi Taniguchi, Jason Alicea, and Stevan Nadj-Perge. Spin-orbit enhanced superconductivity in bernal bilayer graphene. *arXiv*, 2022. doi: 10.48550/ARXIV.2205.05087. URL <https://arxiv.org/abs/2205.05087>.

- ⁶ F. Guinea. Superconductivity and other phases in graphene multilayers, without twists. *Journal Club for Condensed Matter Physics*, 2021. doi: https://doi.org/10.36471/JCCM_November_2021_01.
- ⁷ J. W. McClure. Electron energy band structure and electronic properties of rhombohedral graphite. *Carbon*, 7:425, 1969. doi: [https://doi.org/10.1016/0008-6223\(69\)90073-6](https://doi.org/10.1016/0008-6223(69)90073-6).
- ⁸ A. H. Castro Neto, F. Guinea, N. M. R. Peres, K. S. Novoselov, and A. K. Geim. The electronic properties of graphene. *Rev. Mod. Phys.*, 81:109–162, Jan 2009. doi: 10.1103/RevModPhys.81.109. URL <https://link.aps.org/doi/10.1103/RevModPhys.81.109>.
- ⁹ K. S. Novoselov, D. Jiang, F. Schedin, T. J. Booth, V. V. Khotkevich, S. V. Morozov, and A. K. Geim. Two-dimensional atomic crystals. *Proc. Nat. Acad. Sci. (USA)*, 102:10451, 2004. doi: 10.1073/pnas.0502848102.
- ¹⁰ K. S. Novoselov, A. K. Geim, S. V. Morozov, D. Jiang, Y. Zhang, S. V. Dubonos, I. V. Grigorieva, and A. A. Firsov. Electric field effect in atomically thin carbon films. *Science*, 306:666, 2004. doi: 10.1126/science.1102.
- ¹¹ J. Gonzalez, F. Guinea, and M. A. H. Vozmediano. Non-fermi liquid behavior of electrons in the half-filled honeycomb lattice (a renormalization group approach). *Nucl. Phys. B*, 424:595, 1994. doi: [https://doi.org/10.1016/0550-3213\(94\)90410-3](https://doi.org/10.1016/0550-3213(94)90410-3).
- ¹² D. C. Elias, R. V. Gorbachev, A. S. Mayorov, S. V. Morozov, A. A. Zhukov, P. Blake, L. A. Ponomarenko, I. V. Grigorieva, K. S. Novoselov, F. Guinea, and A. K. Geim. Dirac cones reshaped by interaction effects in suspended graphene. *Nature Phys.*, 7:701, 2011. doi: <https://doi.org/10.1038/nphys2049>.
- ¹³ Y. Zhang, Z. Jiang, J. P. Small, M. S. Purewal, Y.-W. Tan, M. Fazlollahi, J. D. Chudow, J. A. Jaszczak, H. L. Stormer, and P. Kim. Landau-level splitting in graphene in high magnetic fields. *Phys. Rev. Lett.*, 96:136806, Apr 2006. doi: 10.1103/PhysRevLett.96.136806. URL <https://link.aps.org/doi/10.1103/PhysRevLett.96.136806>.
- ¹⁴ M. O. Goerbig. Electronic properties of graphene in a strong magnetic field. *Rev. Mod. Phys.*, 83:1193–1243, Nov 2011. doi: 10.1103/RevModPhys.83.1193. URL <https://link.aps.org/doi/10.1103/RevModPhys.83.1193>.
- ¹⁵ Edward McCann and Vladimir I. Fal’ko. Landau-level degeneracy and quantum hall effect in a graphite bilayer. *Phys. Rev. Lett.*, 96:086805, Mar 2006. doi: 10.1103/PhysRevLett.96.086805. URL <https://link.aps.org/doi/10.1103/PhysRevLett.96.086805>.
- ¹⁶ M. Koshino and E. McCann. The electronic properties of bilayer graphene. *Rep. Prog. Phys.*, 73:057503, 2013. doi: <https://doi.org/10.1088/0034-4885/76/5/056503>.
- ¹⁷ Johan Nilsson, A. H. Castro Neto, N. M. R. Peres, and F. Guinea. Electron-electron interactions and the phase diagram of a graphene bilayer. *Phys. Rev. B*, 73:214418, Jun 2006. doi: 10.1103/PhysRevB.73.214418. URL <https://link.aps.org/doi/10.1103/PhysRevB.73.214418>.
- ¹⁸ Hongki Min, Giovanni Borghi, Marco Polini, and A. H. MacDonald. Pseudospin magnetism in graphene. *Phys. Rev. B*, 77:041407, Jan 2008. doi: 10.1103/PhysRevB.77.041407. URL <https://link.aps.org/doi/10.1103/PhysRevB.77.041407>.
- ¹⁹ Oskar Vafek. Interacting fermions on the honeycomb bilayer: From weak to strong coupling. *Phys. Rev. B*, 82:205106, Nov 2010. doi: 10.1103/PhysRevB.82.205106. URL <https://link.aps.org/doi/10.1103/PhysRevB.82.205106>.
- ²⁰ Rahul Nandkishore and Leonid Levitov. Dynamical screening and excitonic instability in bilayer graphene. *Phys. Rev. Lett.*, 104:156803, Apr 2010. doi: 10.1103/PhysRevLett.104.156803. URL <https://link.aps.org/doi/10.1103/PhysRevLett.104.156803>.
- ²¹ Y. Lemonik, I. Aleiner, and V. I. Fal’ko. Competing nematic, antiferromagnetic, and spin-flux orders in the ground state of bilayer graphene. *Phys. Rev. B*, 85:245451, Jun 2012. doi: 10.1103/PhysRevB.85.245451. URL <https://link.aps.org/doi/10.1103/PhysRevB.85.245451>.
- ²² Rahul Nandkishore, Leonid Levitov, and Andrey Chubukov. Chiral superconductivity from repulsive interactions in doped graphene. *Nature Phys.*, 8:158, 2012. doi: <https://doi.org/10.1038/nphys2208>.
- ²³ J. L. McChesney, Aaron Bostwick, Taisuke Ohta, Thomas Seyller, Karsten Horn, J. González, and Eli Rotenberg. Extended van hove singularity and superconducting instability in doped graphene. *Phys. Rev. Lett.*, 104:136803, Apr 2010. doi: 10.1103/PhysRevLett.104.136803. URL <https://link.aps.org/doi/10.1103/PhysRevLett.104.136803>.
- ²⁴ Mikito Koshino. Interlayer screening effect in graphene multilayers with *aba* and *abc* stacking. *Phys. Rev. B*, 81:125304, Mar 2010. doi: 10.1103/PhysRevB.81.125304. URL <https://link.aps.org/doi/10.1103/PhysRevB.81.125304>.
- ²⁵ N. P. Armitage, E. J. Mele, and Ashvin Vishwanath. Weyl and dirac semimetals in three-dimensional solids. *Rev. Mod. Phys.*, 90:015001, Jan 2018. doi: 10.1103/RevModPhys.90.015001. URL <https://link.aps.org/doi/10.1103/RevModPhys.90.015001>.
- ²⁶ Betül Pamuk, Jacopo Baima, Francesco Mauri, and Matteo Calandra. Magnetic gap opening in rhombohedral-stacked multilayer graphene from first principles. *Phys. Rev. B*, 95:075422, Feb 2017. doi: 10.1103/PhysRevB.95.075422. URL <https://link.aps.org/doi/10.1103/PhysRevB.95.075422>.
- ²⁷ Fan Zhang, Bhagawan Sahu, Hongki Min, and A. H. MacDonald. Band structure of *abc*-stacked graphene trilayers. *Phys. Rev. B*, 82:035409, Jul 2010. doi: 10.1103/PhysRevB.82.035409. URL <https://link.aps.org/doi/10.1103/PhysRevB.82.035409>.
- ²⁸ Sergey Slizovskiy, Edward McCann, Mikito Koshino, and Vladimir I. Fal’ko. Films of rhombohedral graphite as two-dimensional topological semimetals. *Commun. in Physics*, 2:164, 2019. doi: <https://doi.org/10.1038/s42005-019-0268-8>.
- ²⁹ F. Guinea, A. H. Castro Neto, and N. M. R. Peres. Electronic states and landau levels in graphene stacks. *Phys. Rev. B*, 73:245426, Jun 2006. doi: 10.1103/PhysRevB.73.245426. URL <https://link.aps.org/doi/10.1103/PhysRevB.73.245426>.
- ³⁰ Daniel P. Arovas and F. Guinea. Stacking faults, bound states, and quantum hall plateaus in crystalline graphite. *Phys. Rev. B*, 78:245416, Dec 2008. doi: 10.1103/PhysRevB.78.245416. URL <https://link.aps.org/doi/10.1103/PhysRevB.78.245416>.
- ³¹ Fan Zhang, Jeil Jung, Gregory A. Fiete, Qian Niu, and Allan H. MacDonald. Spontaneous quantum hall states in chirally stacked few-layer graphene systems. *Phys. Rev. Lett.*, 106:156801, Apr 2011. doi: 10.1103/PhysRevLett.106.156801. URL

- <https://link.aps.org/doi/10.1103/PhysRevLett.106.156801>.
- ³² James H. Muten, Alex J. Copeland, and Edward McCann. Exchange interaction, disorder, and stacking faults in rhombohedral graphene multilayers. *Phys. Rev. B*, 104:035404, Jul 2021. doi: 10.1103/PhysRevB.104.035404. URL <https://link.aps.org/doi/10.1103/PhysRevB.104.035404>.
- ³³ Aitor Garcia-Ruiz, Sergey Slizovskiy, and Vladimir I. Fal'ko. Electronic properties of rhombohedral graphene multilayers with a twin boundary. *arXiv*, 2022. doi: 10.48550/ARXIV.2210.07610. URL <https://arxiv.org/abs/2210.07610>.
- ³⁴ N. B. Kopnin, T. T. Heikkilä, and G. E. Volovik. High-temperature surface superconductivity in topological flat-band systems. *Phys. Rev. B*, 83:220503, Jun 2011. doi: 10.1103/PhysRevB.83.220503. URL <https://link.aps.org/doi/10.1103/PhysRevB.83.220503>.
- ³⁵ N. B. Kopnin, M. Ijäs, A. Harju, and T. T. Heikkilä. High-temperature surface superconductivity in rhombohedral graphite. *Phys. Rev. B*, 87:140503, Apr 2013. doi: 10.1103/PhysRevB.87.140503. URL <https://link.aps.org/doi/10.1103/PhysRevB.87.140503>.
- ³⁶ G. E. Volovik. Graphite, graphene, and the flat band superconductivity. *JETP Lett.*, 107:516, 2018. doi: <https://doi.org/10.1134/S0021364018080052>.
- ³⁷ M. S. Dresselhaus and G. Dresselhaus. Intercalation compounds of graphite. *Adv. in Phys.*, 51:1, 2002. doi: 10.1080/00018738100101367.
- ³⁸ Robert P. Smith, Thomas E. Weller, Christopher A. Howard, Mark P.M. Dean, Kaveh C. Rahnejat, Siddharth S. Saxena, and Mark Ellerby. Superconductivity in graphite intercalation compounds. *Physica C: Superconductivity and its Applications*, 514:50–58, 2015. ISSN 0921-4534. doi: <https://doi.org/10.1016/j.physc.2015.02.029>. URL <https://www.sciencedirect.com/science/article/pii/S0921453415000568>. Superconducting Materials: Conventional, Unconventional and Undetermined.
- ³⁹ Y. Takada. Theory of superconductivity in graphite intercalation compounds. In *Reference Module in Materials Science and Materials Engineering*. Elsevier, 2016. doi: 10.1016/b978-0-12-803581-8.00774-8. URL <https://doi.org/10.1016/b978-0-12-803581-8.00774-8>.
- ⁴⁰ M. J. Rosseinsky, A. P. Ramirez, S. H. Glarum, D. W. Murphy, R. C. Haddon, A. F. Hebard, T. T. M. Palstra, A. R. Kortan, S. M. Zahurak, and A. V. Makhija. Superconductivity at 28 k in rb_xc_{60} . *Phys. Rev. Lett.*, 66:2830–2832, May 1991. doi: 10.1103/PhysRevLett.66.2830. URL <https://link.aps.org/doi/10.1103/PhysRevLett.66.2830>.
- ⁴¹ Stephen P. Kelty, Chia-Chun Chen, and Charles M. Lieber. Superconductivity at 30 k in caesium-doped c_{60} . *Nature*, 352(6332):223–225, July 1991. doi: 10.1038/352223a0. URL <https://doi.org/10.1038/352223a0>.
- ⁴² S Chakravarty and S Kivelson. Superconductivity of doped fullerenes. *Europhysics Letters (EPL)*, 16(8):751–756, October 1991. doi: 10.1209/0295-5075/16/8/008. URL <https://doi.org/10.1209/0295-5075/16/8/008>.
- ⁴³ A. F. Hebard, M. J. Rosseinsky, R. C. Haddon, D. W. Murphy, S. H. Glarum, T. T. M. Palstra, A. P. Ramirez, and A. R. Kortan. Superconductivity at 18 k in potassium-doped c_{60} . *Nature*, 350(6319):600–601, April 1991. doi: 10.1038/350600a0. URL <https://doi.org/10.1038/350600a0>.
- ⁴⁴ A. F. Hebard. Superconductivity in doped fullerenes. *Physics Today*, 45:26, 1992. doi: <https://doi.org/10.1063/1.881320>.
- ⁴⁵ M. Capone, M. Fabrizio, C. Castellani, and E. Tosatti. Strongly correlated superconductivity. *Science*, 296:2634, 2002. doi: 10.1126/science.107112.
- ⁴⁶ Yusuke Nomura, Shiro Sakai, Massimo Capone, and Ryotaro Arita. Unified understanding of superconductivity and mott transition in alkali-doped fullerides from first principles. *Sci. Adv.*, 7:1:e1500568, 2015. doi: 10.1126/sciadv.1500568.
- ⁴⁷ Matteo Calandra and Francesco Mauri. Theoretical explanation of superconductivity in C_6Ca . *Phys. Rev. Lett.*, 95:237002, Nov 2005. doi: 10.1103/PhysRevLett.95.237002. URL <https://link.aps.org/doi/10.1103/PhysRevLett.95.237002>.
- ⁴⁸ G. Wang, W. R. Datars, and P. K. Ummat. Fermi surface of the stage-1 potassium graphite intercalation compound. *Phys. Rev. B*, 44:8294–8300, Oct 1991. doi: 10.1103/PhysRevB.44.8294. URL <https://link.aps.org/doi/10.1103/PhysRevB.44.8294>.
- ⁴⁹ A. Cantaluppi, M. Buzzi, G. Jotzu, D. Nicoletti, M. Mitranò, D. Pontiroli, M. Riccò, A. Perucchi, P. Di Pietro, and A. Cavalleri. Pressure tuning of light-induced superconductivity in k_3c_{60} . *Nature Physics*, 14(8):837–841, May 2018. doi: 10.1038/s41567-018-0134-8. URL <https://doi.org/10.1038/s41567-018-0134-8>.
- ⁵⁰ R.C. Haddon, L.E. Brus, and Krishnan Raghavachari. Electronic structure and bonding in icosahedral c_{60} . *Chemical Physics Letters*, 125(5-6):459–464, April 1986. doi: 10.1016/0009-2614(86)87079-8. URL [https://doi.org/10.1016/0009-2614\(86\)87079-8](https://doi.org/10.1016/0009-2614(86)87079-8).
- ⁵¹ Steven C. Erwin and Warren E. Pickett. Theoretical fermi-surface properties and superconducting parameters for k_3c_{60} . *Science*, 254(5033):842–845, November 1991. doi: 10.1126/science.254.5033.842. URL <https://doi.org/10.1126/science.254.5033.842>.
- ⁵² R. Thomas Weitz, Monica T. Allen, Benjamin E. Feldman, Jens Martin, and Amir Yacoby. Coulomb-driven broken-symmetry states in doubly gated suspended bilayer graphene. *Science*, 330:812, 2010. doi: 10.1126/science.1194988.
- ⁵³ F. Freitag, J. Trbovic, M. Weiss, and C. Schönenberger. Spontaneously gapped ground state in suspended bilayer graphene. *Phys. Rev. Lett.*, 108:076602, Feb 2012. doi: 10.1103/PhysRevLett.108.076602. URL <https://link.aps.org/doi/10.1103/PhysRevLett.108.076602>.
- ⁵⁴ Wenzhong Bao, Jairo Velasco Jr, Fan Zhang, Lei Jing, Brian Standley, Dmitry Smirnov, Marc Bockrath, Allan MacDonald, and Chun Ning Lau. Minimum conductivity and evidence for phase transitions in ultra-clean bilayer graphene. *Proc. Nat. Acad. Sci. (USA)*, 109:10802, 2012. doi: <https://doi.org/10.1073/pnas.120597810>.
- ⁵⁵ Anastasia Varlet, Dominik Bischoff, Pauline Simonet, Kenji Watanabe, Takashi Taniguchi, Thomas Ihn, Klaus Ensslin, Marcin Mucha-Kruczyński, and Vladimir I. Fal'ko. Anomalous sequence of quantum hall liquids revealing a tunable lifshitz transition in bilayer graphene. *Phys. Rev. Lett.*, 113:116602, Sep 2014. doi: 10.1103/PhysRevLett.113.116602. URL

- <https://link.aps.org/doi/10.1103/PhysRevLett.113.116602>.
- ⁵⁶ Kayoung Lee, Babak Fallahazad, Jiamin Xue, David C. Dillen, Kyoungwan Kim, Takashi Taniguchi, Kenji Watanabe, and Emanuel Tutuc. Chemical potential and quantum hall ferromagnetism in bilayer graphene. *Science*, 345:58, 2014. doi: 10.1126/science.1251003.
- ⁵⁷ Satoshi Moriyama, Yoshifumi Morita, Katsuyoshi Komatsu, Kosuke Endo, Takuya Iwasaki, Shu Nakaharai, Yutaka Noguchi, Yutaka Wakayama, Eiichiro Watanabe, Daiju Tsuya, Kenji Watanabe, and Takashi Taniguchi. Observation of superconductivity in bilayer graphene/hexagonal boron nitride superlattices. 2019. doi: 10.48550/ARXIV.1901.09356. URL <https://arxiv.org/abs/1901.09356>.
- ⁵⁸ Guorui Chen, Aaron L. Sharpe, Patrick Gallagher, Ilan T. Rosen, Eli J. Fox, Lili Jiang, Bosai Lyu, Hongyuan Li, Kenji Watanabe, Takashi Taniguchi, Jeil Jung, Zhiwen Shi, David Goldhaber-Gordon, Yuanbo Zhang, and Feng Wang. Signatures of tunable superconductivity in a trilayer graphene moiré superlattice. *Nature*, 572(7768):215–219, July 2019. doi: 10.1038/s41586-019-1393-y. URL <https://doi.org/10.1038/s41586-019-1393-y>.
- ⁵⁹ Guorui Chen, Lili Jiang, Shuang Wu, Bosai Lyu, Hongyuan Li, Bheema Lingam Chittari, Kenji Watanabe, Takashi Taniguchi, Zhiwen Shi, Jeil Jung, Yuanbo Zhang, and Feng Wang. Evidence of a gate-tunable mott insulator in a trilayer graphene moiré superlattice. *Nature Physics*, 15(3):237–241, January 2019. doi: 10.1038/s41567-018-0387-2. URL <https://doi.org/10.1038/s41567-018-0387-2>.
- ⁶⁰ Guorui Chen, Aaron L. Sharpe, Eli J. Fox, Ya-Hui Zhang, Shaoxin Wang, Lili Jiang, Bosai Lyu, Hongyuan Li, Kenji Watanabe, Takashi Taniguchi, Zhiwen Shi, T. Senthil, David Goldhaber-Gordon, Yuanbo Zhang, and Feng Wang. Tunable correlated chern insulator and ferromagnetism in a moiré superlattice. *Nature*, 579(7797):56–61, March 2020. doi: 10.1038/s41586-020-2049-7. URL <https://doi.org/10.1038/s41586-020-2049-7>.
- ⁶¹ P. San-Jose, R. V. Gorbachev, A. K. Geim, K. S. Novoselov, and F. Guinea. Stacking boundaries and transport in bilayer graphene. *Nano Lett.*, 14:2052, 2014. doi: <https://doi.org/10.1021/nl500230a>.
- ⁶² Y. Lee, D. Tran, K. Myhro, J. Velasco, N. Gillgren, C. N. Lau, Y. Barlas, J. M. Poumirol, D. Smirnov, and F. Guinea. Competition between spontaneous symmetry breaking and single-particle gaps in trilayer graphene. *Nature Comm.*, 5:5656, 2014. doi: <https://doi.org/10.1038/ncomms6656>.
- ⁶³ A. A. Zibrov, P. Rao, C. Kometter, E. M. Spanton, J. I. A. Li, Cory R. Dean, T. Taniguchi, K. Watanabe, M. Serbyn, and A. F. Young. Emergent dirac gullies and gully-symmetry-breaking quantum hall states in *aba* trilayer graphene. *Phys. Rev. Lett.*, 121:167601, Oct 2018. doi: 10.1103/PhysRevLett.121.167601. URL <https://link.aps.org/doi/10.1103/PhysRevLett.121.167601>.
- ⁶⁴ Youngwoo Nam, Dong-Keun Ki, Mikito Koshino, Edward McCann, and Alberto F. Morpurgo. Interaction-induced insulating state in thick multilayer graphene. *2D Mater.*, 3:045014, 2016. doi: 10.1088/2053-1583/3/4/045014.
- ⁶⁵ Youngwoo Nam, Dong-Keun Ki, David Soler-Delgado, and Alberto F. Morpurgo. A family of finite-temperature electronic phase transitions in graphene multilayers. *Science*, 362:324, 2018. doi: 10.1126/science.aar68.
- ⁶⁶ Alexander Kerelsky, Carmen Rubio-Verdú, Lede Xian, Dorri Halbertal Dante M. Kennes, Nathan Finney, Larry Song, Simon Turkel, Lei Wang, Kenji Watanabe, Takashi Taniguchi, James Hone, Cory Dean, Dmitri N. Basov, Angel Rubio, and Abhay N. Pasupathy. Moiréless correlations in abca graphene. *Proc. Nat. Acad. Sci. (USA)*, 118:e2017366118, 2021. doi: <https://doi.org/10.1073/pnas.2017366118>.
- ⁶⁷ P. Esquinazi. Invited review: Graphite and its hidden superconductivity. *Papers in Physics*, 5:050007, 2013. URL <https://doi.org/10.4279/pip.050007>.
- ⁶⁸ P. Esquinazi, T. T. Heikkilä, Y. V. Lysogorskiy, D. A. Tayurskii, and G. E. Volovik. On the superconductivity of graphite interfaces. *JETP Lett.*, 100:336, 2014. doi: <https://doi.org/10.1134/S0021364014170056>.
- ⁶⁹ Pablo D. Esquinazi, Christian E. Precker, Markus Stiller, Tiago R. S. Cordeiro, Jose Barzola-Quiquia, Annette Setzer, and Winfried Böhlmann. Evidence for room temperature superconductivity at graphite interfaces. *Quantum Stud.: Math. Found.*, 5:41, 2018. doi: <https://doi.org/10.1007/s40509-017-0131-0>.
- ⁷⁰ P. D. Esquinazi. Ordered defects: A roadmap towards room temperature superconductivity and magnetic order. *arXiv*, 2019. doi: <https://doi.org/10.48550/arXiv.1902.07489>.
- ⁷¹ T. Scheike, W. Böhlmann, P. Esquinazi, J. Barzola-Quiquia, A. Ballestar, and A. Setzer. Can doping graphite trigger room temperature superconductivity? evidence for granular high-temperature superconductivity in water-treated graphite powder. *Advanced Materials*, 24(43):5826–5831, September 2012. doi: 10.1002/adma.201202219. URL <https://doi.org/10.1002/adma.201202219>.
- ⁷² Samar Layek, Miguel Monteverde, Gastón Garbarino, Marie-Aude Méasson, André Sulpice, Nedjma Bendiab, Pierre Rodière, Romain Cazali, Abdellali Hadj-Azzem, Vivian Nassif, Daniel Bourgault, Frédéric Gay, Didier Dufeu, Sébastien Pairis, Jean-Louis Hodeau, and Manuel Núñez-Regueiro. Possible high temperature superconducting transitions in disordered graphite obtained from room temperature deintercalated kcs. *arXiv*, 2022. doi: 10.48550/ARXIV.2205.09358. URL <https://arxiv.org/abs/2205.09358>.
- ⁷³ Regina Ariskina, Markus Stiller, Christian E. Precker, Winfried Böhlmann, and Pablo D. Esquinazi. On the localization of persistent currents due to trapped magnetic flux at the stacking faults of graphite at room temperature. *Materials*, 15(10):3422, May 2022. doi: 10.3390/ma15103422. URL <https://doi.org/10.3390/ma15103422>.
- ⁷⁴ Raphael Rousset-Zenou, Samar Layek, Miguel Monteverde, Frédéric Gay, Didier Dufeu, and Manuel Núñez-Regueiro. Hidden granular superconductivity above 500k in off-the-shelf graphite materials. 2022. doi: 10.48550/ARXIV.2207.09149. URL <https://arxiv.org/abs/2207.09149>.
- ⁷⁵ Kai Yan, Hailin Peng, Yu Zhou, Hui Li, and Zhongfan Liu. Formation of bilayer bernal graphene: Layer-by-layer epitaxy via chemical vapor deposition. *Nano Letters*, 11(3):1106–1110, February 2011. doi: 10.1021/nl104000b. URL <https://doi.org/10.1021/nl104000b>.

- ⁷⁶ Seunghyun Lee, Kyunghoon Lee, and Zhaohui Zhong. Wafer scale homogeneous bilayer graphene films by chemical vapor deposition. *Nano Letters*, 10(11):4702–4707, October 2010. doi: [10.1021/nl1029978](https://doi.org/10.1021/nl1029978). URL <https://doi.org/10.1021/nl1029978>.
- ⁷⁷ Uri Zondiner, Asaf Rozen, Daniel Rodan-Legrain, Yuan Cao, Raquel Queiroz, Takashi Taniguchi, Kenji Watanabe, Yuval Oreg, Felix von Oppen, Ady Stern, E. Berg, P. Jarillo-Herrero, and S. Ilani. Cascade of phase transitions and dirac revivals in magic-angle graphene. *Nature*, 582(7811):203–208, 2020. doi: <https://doi.org/10.1038/s41586-020-2373-y>.
- ⁷⁸ Dillon Wong, Kevin P Nuckolls, Myungchul Oh, Biao Lian, Yonglong Xie, Sangjun Jeon, Kenji Watanabe, Takashi Taniguchi, B Andrei Bernevig, and Ali Yazdani. Cascade of electronic transitions in magic-angle twisted bilayer graphene. *Nature*, 582(7811):198–202, 2020. doi: <https://doi.org/10.1038/s41586-020-2339-0>.
- ⁷⁹ Youngjoon Choi, Hyunjin Kim, Yang Peng, Alex Thomson, Cyprian Lewandowski, Robert Polski, Yiran Zhang, Harpreet Singh Arora, Kenji Watanabe, Takashi Taniguchi, Jason Alicea, and Stevan Nadj-Perge. Correlation-driven topological phases in magic-angle twisted bilayer graphene. *Nature*, 589(7843):536–541, 2021. doi: <https://doi.org/10.1038/s41586-020-03159-7>.
- ⁸⁰ Haoxin Zhou, Tian Xie, Areg Ghazaryan, Tobias Holder, James R. Ehrets, Eric M. Spanton, Takashi Taniguchi, Kenji Watanabe, Erez Berg, Maksym Serbyn, and Andrea F. Young. Half- and quarter-metals in rhombohedral trilayer graphene. *Nature*, 598(7881):429–433, oct 2021. ISSN 14764687. doi: [10.1038/s41586-021-03938-w](https://doi.org/10.1038/s41586-021-03938-w).
- ⁸¹ Sergio C de la Barrera, Samuel Aranson, Zhiren Zheng, Kenji Watanabe, Takashi Taniguchi, Qiong Ma, Pablo Jarillo-Herrero, and Raymond Ashoori. Cascade of isospin phase transitions in bernal-stacked bilayer graphene at zero magnetic field. *Nature Physics*, pages 1–5, 2022. doi: <https://doi.org/10.1038/s41567-022-01616-w>.
- ⁸² Anna M Seiler, Fabian R Geisenhof, Felix Winterer, Kenji Watanabe, Takashi Taniguchi, Tianyi Xu, Fan Zhang, and R Thomas Weitz. Quantum cascade of correlated phases in trigonally warped bilayer graphene. *Nature*, 608(7922):298–302, 2022. doi: <https://doi.org/10.1038/s41586-022-04937-1>.
- ⁸³ Harpreet Singh Arora, Robert Polski, Yiran Zhang, Alex Thomson, Youngjoon Choi, Hyunjin Kim, Zhong Lin, Ilham Zaky Wilson, Xiaodong Xu, Jiun-Haw Chu, Kenji Watanabe, Takashi Taniguchi, Jason Alicea, and Stevan Nadj-Perge. Superconductivity in metallic twisted bilayer graphene stabilized by wse_2 . *Nature*, 583(7816):379–384, 2020. doi: <https://doi.org/10.1038/s41586-020-2473-8>.
- ⁸⁴ S. Konschuh, M. Gmitra, D. Kochan, and J. Fabian. Theory of spin-orbit coupling in bilayer graphene. *Phys. Rev. B*, 85: 115423, Mar 2012. doi: [10.1103/PhysRevB.85.115423](https://doi.org/10.1103/PhysRevB.85.115423). URL <https://link.aps.org/doi/10.1103/PhysRevB.85.115423>.
- ⁸⁵ Martin Gmitra and Jaroslav Fabian. Proximity effects in bilayer graphene on monolayer wse_2 : Field-effect spin valley locking, spin-orbit valve, and spin transistor. *Phys. Rev. Lett.*, 119:146401, Oct 2017. doi: [10.1103/PhysRevLett.119.146401](https://doi.org/10.1103/PhysRevLett.119.146401). URL <https://link.aps.org/doi/10.1103/PhysRevLett.119.146401>.
- ⁸⁶ Jun Yong Khoo, Alberto F Morpurgo, and Leonid Levitov. On-demand spin-orbit interaction from which-layer tunability in bilayer graphene. *Nano letters*, 17(11):7003–7008, 2017. doi: <https://doi.org/10.1021/acs.nanolett.7b03604>.
- ⁸⁷ Raúl Guerrero-Avilés, Marta Pelc, Fabian Geisenhof, Thomas Weitz, and Andrés Ayuela. Relative stability of bernal and rhombohedral stackings in trilayer graphene under distortions. *arXiv*, 2021. doi: [10.48550/ARXIV.2110.06590](https://doi.org/10.48550/ARXIV.2110.06590). URL <https://arxiv.org/abs/2110.06590>.
- ⁸⁸ Tommaso Cea, Pierre A. Pantaleón, Niels R. Walet, and Francisco Guinea. Electrostatic interactions in twisted bilayer graphene. *Nano Materials Science*, 4:27, 2022.
- ⁸⁹ Jeong Min Park, Yuan Cao, Kenji Watanabe, Takashi Taniguchi, and Pablo Jarillo-Herrero. Tunable strongly coupled superconductivity in magic-angle twisted trilayer graphene. *Nature*, 590(7845):249–255, February 2021. doi: [10.1038/s41586-021-03192-0](https://doi.org/10.1038/s41586-021-03192-0). URL <https://doi.org/10.1038/s41586-021-03192-0>.
- ⁹⁰ Zeyu Hao, A. M. Zimmerman, Patrick Ledwith, Eslam Khalaf, Danial Haie Najafabadi, Kenji Watanabe, Takashi Taniguchi, Ashvin Vishwanath, and Philip Kim. Electric field-tunable superconductivity in alternating-twist magic-angle trilayer graphene. *Science*, 371(6534):1133–1138, March 2021. doi: [10.1126/science.abg0399](https://doi.org/10.1126/science.abg0399). URL <https://doi.org/10.1126/science.abg0399>.
- ⁹¹ Yuan Cao, Jeong Min Park, Kenji Watanabe, Takashi Taniguchi, and Pablo Jarillo-Herrero. Pauli-limit violation and re-entrant superconductivity in moiré graphene. *Nature*, 595(7868):526–531, July 2021. doi: [10.1038/s41586-021-03685-y](https://doi.org/10.1038/s41586-021-03685-y). URL <https://doi.org/10.1038/s41586-021-03685-y>.
- ⁹² Yiran Zhang, Robert Polski, Cyprian Lewandowski, Alex Thomson, Yang Peng, Youngjoon Choi, Hyunjin Kim, Kenji Watanabe, Takashi Taniguchi, Jason Alicea, Felix von Oppen, Gil Refael, and Stevan Nadj-Perge. Promotion of superconductivity in magic-angle graphene multilayers. *Science*, 377(6614):1538–1543, September 2022. doi: [10.1126/science.abn8585](https://doi.org/10.1126/science.abn8585). URL <https://doi.org/10.1126/science.abn8585>.
- ⁹³ Jeong Min Park, Yuan Cao, Li-Qiao Xia, Shuwen Sun, Kenji Watanabe, Takashi Taniguchi, and Pablo Jarillo-Herrero. Robust superconductivity in magic-angle multilayer graphene family. *Nature Materials*, 21(8):877–883, July 2022. doi: [10.1038/s41563-022-01287-1](https://doi.org/10.1038/s41563-022-01287-1). URL <https://doi.org/10.1038/s41563-022-01287-1>.
- ⁹⁴ M. Serlin, C. L. Tschirhart, H. Polshyn, Y. Zhang, J. Zhu, K. Watanabe, T. Taniguchi, L. Balents, and A. F. Young. Intrinsic quantized anomalous hall effect in a moiré heterostructure. *Science*, 367(6480):900–903, February 2020. doi: [10.1126/science.aay5533](https://doi.org/10.1126/science.aay5533). URL <https://doi.org/10.1126/science.aay5533>.
- ⁹⁵ Hryhoriy Polshyn, Matthew Yankowitz, Shaowen Chen, Yuxuan Zhang, K. Watanabe, T. Taniguchi, Cory R. Dean, and Andrea F. Young. Large linear-in-temperature resistivity in twisted bilayer graphene. *Nature Physics*, 15(10):1011–1016, August 2019. doi: [10.1038/s41567-019-0596-3](https://doi.org/10.1038/s41567-019-0596-3). URL <https://doi.org/10.1038/s41567-019-0596-3>.
- ⁹⁶ Guorui Chen, Aaron L. Sharpe, Eli J. Fox, Ya-Hui Zhang, Shaoxin Wang, Lili Jiang, Bosai Lyu, Hongyuan Li, Kenji Watanabe, Takashi Taniguchi, Zhiwen Shi, T. Senthil, David Goldhaber-Gordon, Yuanbo Zhang, and Feng Wang. Tunable correlated chern insulator and ferromagnetism in a moiré superlattice. *Nature*, 579(7797):56–61, March 2020. doi: [10.1038](https://doi.org/10.1038)

- s41586-020-2049-7. URL <https://doi.org/10.1038/s41586-020-2049-7>.
- ⁹⁷ Kevin P. Nuckolls, Myungchul Oh, Dillon Wong, Biao Lian, Kenji Watanabe, Takashi Taniguchi, B. Andrei Bernevig, and Ali Yazdani. Strongly correlated chern insulators in magic-angle twisted bilayer graphene. *Nature*, 588(7839):610–615, December 2020. doi: 10.1038/s41586-020-3028-8. URL <https://doi.org/10.1038/s41586-020-3028-8>.
- ⁹⁸ Yu Saito, Jingyuan Ge, Louk Rademaker, Kenji Watanabe, Takashi Taniguchi, Dmitry A. Abanin, and Andrea F. Young. Hofstadter subband ferromagnetism and symmetry-broken chern insulators in twisted bilayer graphene. *Nature Physics*, 17(4):478–481, January 2021. doi: 10.1038/s41567-020-01129-4. URL <https://doi.org/10.1038/s41567-020-01129-4>.
- ⁹⁹ Shuang Wu, Zhenyuan Zhang, K. Watanabe, T. Taniguchi, and Eva Y. Andrei. Chern insulators, van hove singularities and topological flat bands in magic-angle twisted bilayer graphene. *Nature Materials*, 20(4):488–494, February 2021. doi: 10.1038/s41563-020-00911-2. URL <https://doi.org/10.1038/s41563-020-00911-2>.
- ¹⁰⁰ Andrew T. Pierce, Yonglong Xie, Jeong Min Park, Eslam Khalaf, Seung Hwan Lee, Yuan Cao, Daniel E. Parker, Patrick R. Forrester, Shaowen Chen, Kenji Watanabe, Takashi Taniguchi, Ashvin Vishwanath, Pablo Jarillo-Herrero, and Amir Yacoby. Unconventional sequence of correlated chern insulators in magic-angle twisted bilayer graphene. *Nature Physics*, 17(11):1210–1215, September 2021. doi: 10.1038/s41567-021-01347-4. URL <https://doi.org/10.1038/s41567-021-01347-4>.
- ¹⁰¹ Petr Stepanov, Ming Xie, Takashi Taniguchi, Kenji Watanabe, Xiaobo Lu, Allan H. MacDonald, B. Andrei Bernevig, and Dmitri K. Efetov. Competing zero-field chern insulators in superconducting twisted bilayer graphene. *Phys. Rev. Lett.*, 127:197701, Nov 2021. doi: 10.1103/PhysRevLett.127.197701. URL <https://link.aps.org/doi/10.1103/PhysRevLett.127.197701>.
- ¹⁰² Yonglong Xie, Andrew T. Pierce, Jeong Min Park, Daniel E. Parker, Eslam Khalaf, Patrick Ledwith, Yuan Cao, Seung Hwan Lee, Shaowen Chen, Patrick R. Forrester, Kenji Watanabe, Takashi Taniguchi, Ashvin Vishwanath, Pablo Jarillo-Herrero, and Amir Yacoby. Fractional chern insulators in magic-angle twisted bilayer graphene. *Nature*, 600(7889):439–443, December 2021. doi: 10.1038/s41586-021-04002-3. URL <https://doi.org/10.1038/s41586-021-04002-3>.
- ¹⁰³ Yuan Cao, Daniel Rodan-Legrain, Jeong Min Park, Noah F. Q. Yuan, Kenji Watanabe, Takashi Taniguchi, Rafael M. Fernandes, Liang Fu, and Pablo Jarillo-Herrero. Nematicity and competing orders in superconducting magic-angle graphene. *Science*, 372(6539):264–271, April 2021. doi: 10.1126/science.abc2836. URL <https://doi.org/10.1126/science.abc2836>.
- ¹⁰⁴ Asaf Rozen, Jeong Min Park, Uri Zondiner, Yuan Cao, Daniel Rodan-Legrain, Takashi Taniguchi, Kenji Watanabe, Yuval Oreg, Ady Stern, Erez Berg, Pablo Jarillo-Herrero, and Shahal Ilani. Entropic evidence for a pomeranchuk effect in magic-angle graphene. *Nature*, 592(7853):214–219, April 2021. doi: 10.1038/s41586-021-03319-3. URL <https://doi.org/10.1038/s41586-021-03319-3>.
- ¹⁰⁵ Yu Saito, Fangyuan Yang, Jingyuan Ge, Xiaoxue Liu, Takashi Taniguchi, Kenji Watanabe, J. I. A. Li, Erez Berg, and Andrea F. Young. Isospin pomeranchuk effect in twisted bilayer graphene. *Nature*, 592(7853):220–224, April 2021. doi: 10.1038/s41586-021-03409-2. URL <https://doi.org/10.1038/s41586-021-03409-2>.
- ¹⁰⁶ Tommaso Cea, Pierre A. Pantaleón, Võ Tién Phong, and Francisco Guinea. Superconductivity from repulsive interactions in rhombohedral trilayer graphene: A kohn-luttinger-like mechanism. *Phys. Rev. B*, 105:075432, Feb 2022. doi: 10.1103/PhysRevB.105.075432. URL <https://link.aps.org/doi/10.1103/PhysRevB.105.075432>.
- ¹⁰⁷ K. S. Novoselov, E. McCann, S. V. Morozov, V. I. Fal’ko, M. I. Katsnelson, U. Zeitler, D. Jiang, F. Schedin, and A. K. Geim. Unconventional quantum hall effect and berry’s phase of 2π in bilayer graphene. *Nature Phys.*, 2:177, 2006. doi: 10.1038/nphys2103. URL <https://doi.org/10.1038/nphys2103>.
- ¹⁰⁸ Fan Zhang and A. H. MacDonald. Distinguishing spontaneous quantum hall states in bilayer graphene. *Phys. Rev. Lett.*, 108:186804, May 2012. doi: 10.1103/PhysRevLett.108.186804. URL <https://link.aps.org/doi/10.1103/PhysRevLett.108.186804>.
- ¹⁰⁹ Vladimir Cvetkovic, Robert E. Throckmorton, and Oskar Vafeek. Electronic multicriticality in bilayer graphene. *Phys. Rev. B*, 86:075467, Aug 2012. doi: 10.1103/PhysRevB.86.075467. URL <https://link.aps.org/doi/10.1103/PhysRevB.86.075467>.
- ¹¹⁰ Jens Martin, Benjamin Ezekiel Feldman, R Thomas Weitz, Monica T Allen, and Amir Yacoby. Local compressibility measurements of correlated states in suspended bilayer graphene. *Physical review letters*, 105(25):256806, 2010.
- ¹¹¹ Yuanbo Zhang, Tsung-Ta Tang, Caglar Girit, Zhao Hao, Michael C Martin, Alex Zettl, Michael F Crommie, Y Ron Shen, and Feng Wang. Direct observation of a widely tunable bandgap in bilayer graphene. *Nature*, 459(7248):820–823, 2009. doi: <https://doi.org/10.1038/nature08105>.
- ¹¹² W. Bao, L. Jing, J. Velasco Jr., Y. Lee, D. Liu, G. and Tran, B. Standley, M. Aykol, S. B. Cronin, D. Smirnov, M. Koshino, E. McCann, M. Bockrath, and C. N. Lau. Stacking-dependent band gap and quantum transport in trilayer graphene. *Nature Physics*, 7:948, 2011. doi: <https://doi.org/10.1038/nphys2103>.
- ¹¹³ Yanmeng Shi, Shuigang Xu, Yaping Yang, Sergey Slizovskiy, Sergey V. Morozov, Seok-Kyun Son, Servet Ozdemir, Ciaran Mullan, Julien Barrier, Jun Yin, Alexey I. Berdyugin, Benjamin A. Piot, Takashi Taniguchi, Kenji Watanabe, Vladimir I. Fal’ko, Kostya S. Novoselov, A. K. Geim, and Artem Mishchenko. Electronic phase separation in multilayer rhombohedral graphite. *Nature*, 584(7820):210–214, August 2020. doi: 10.1038/s41586-020-2568-2. URL <https://doi.org/10.1038/s41586-020-2568-2>.
- ¹¹⁴ Yang-Zhi Chou, Fengcheng Wu, Jay D. Sau, and Sankar Das Sarma. Acoustic-phonon-mediated superconductivity in bernal bilayer graphene. *Phys. Rev. B*, 105:L100503, Mar 2022. doi: 10.1103/PhysRevB.105.L100503. URL <https://link.aps.org/doi/10.1103/PhysRevB.105.L100503>.
- ¹¹⁵ Yang-Zhi Chou, Fengcheng Wu, Jay D. Sau, and Sankar Das Sarma. Acoustic-phonon-mediated superconductivity in moiréless graphene multilayers. *Phys. Rev. B*, 106:024507, Jul 2022. doi: 10.1103/PhysRevB.106.024507. URL <https://link.aps.org/doi/10.1103/PhysRevB.106.024507>.

- ¹¹⁶ The superconductivity in this model is assumed to emerge from a spin polarized normal state.
- ¹¹⁷ András L. Szabó and Bitan Roy. Competing orders and cascade of degeneracy lifting in doped bernal bilayer graphene. *Phys. Rev. B*, 105:L201107, May 2022. doi: 10.1103/PhysRevB.105.L201107. URL <https://link.aps.org/doi/10.1103/PhysRevB.105.L201107>.
- ¹¹⁸ Zhiyu Dong, Andrey V. Chubukov, and Leonid Levitov. Spin-triplet superconductivity at the onset of isospin order in biased bilayer graphene. 2022. doi: 10.48550/ARXIV.2205.13353. URL <https://arxiv.org/abs/2205.13353>.
- ¹¹⁹ Alejandro Jimeno-Pozo, Héctor Sainz-Cruz, Tommaso Cea, Pierre A. Pantaleón, and Francisco Guinea. Superconductivity from electronic interactions and spin-orbit enhancement in bilayer and trilayer graphene. 2022. doi: 10.48550/ARXIV.2210.02915. URL <https://arxiv.org/abs/2210.02915>.
- ¹²⁰ Tommaso Cea. Superconductivity induced by the intervalley coulomb scattering in a few layers of graphene. *Phys. Rev. B*, 107:L041111, Jan 2023. doi: 10.1103/PhysRevB.107.L041111. URL <https://link.aps.org/doi/10.1103/PhysRevB.107.L041111>.
- ¹²¹ Yang-Zhi Chou, Fengcheng Wu, and Sankar Das Sarma. Enhanced superconductivity through virtual tunneling in bernal bilayer graphene coupled to wse₂. *Phys. Rev. B*, 106:L180502, Nov 2022. doi: 10.1103/PhysRevB.106.L180502. URL <https://link.aps.org/doi/10.1103/PhysRevB.106.L180502>.
- ¹²² Yang-Zhi Chou, Fengcheng Wu, Jay D. Sau, and Sankar Das Sarma. Acoustic-phonon-mediated superconductivity in rhombohedral trilayer graphene. *Phys. Rev. Lett.*, 127:187001, Oct 2021. doi: 10.1103/PhysRevLett.127.187001. URL <https://link.aps.org/doi/10.1103/PhysRevLett.127.187001>.
- ¹²³ András L. Szabó and Bitan Roy. Metals, fractional metals, and superconductivity in rhombohedral trilayer graphene. *Phys. Rev. B*, 105:L081407, Feb 2022. doi: 10.1103/PhysRevB.105.L081407. URL <https://link.aps.org/doi/10.1103/PhysRevB.105.L081407>.
- ¹²⁴ Zhiyu Dong and Leonid Levitov. Superconductivity in the vicinity of an isospin-polarized state in a cubic dirac band. *arXiv*, 2021. doi: 10.48550/ARXIV.2109.01133. URL <https://arxiv.org/abs/2109.01133>.
- ¹²⁵ Shubhayu Chatterjee, Taige Wang, Erez Berg, and Michael P. Zaletel. Inter-valley coherent order and isospin fluctuation mediated superconductivity in rhombohedral trilayer graphene. *Nature Communications*, 13(1), October 2022. doi: 10.1038/s41467-022-33561-w. URL <https://doi.org/10.1038/s41467-022-33561-w>.
- ¹²⁶ Yi-Zhuang You and Ashvin Vishwanath. Kohn-luttinger superconductivity and intervalley coherence in rhombohedral trilayer graphene. *Phys. Rev. B*, 105:134524, Apr 2022. doi: 10.1103/PhysRevB.105.134524. URL <https://link.aps.org/doi/10.1103/PhysRevB.105.134524>.
- ¹²⁷ Tommaso Cea, Pierre A. Pantaleón, Võ Tién Phong, and Francisco Guinea. Superconductivity from repulsive interactions in rhombohedral trilayer graphene: A kohn-luttinger-like mechanism. *Phys. Rev. B*, 105:075432, Feb 2022. doi: 10.1103/PhysRevB.105.075432. URL <https://link.aps.org/doi/10.1103/PhysRevB.105.075432>.
- ¹²⁸ Wei Qin, Chunli Huang, Tobias Wolf, Nemin Wei, Igor Blinov, and Allan H. MacDonald. Functional renormalization group study of superconductivity in rhombohedral trilayer graphene. *arXiv*, 2022. doi: 10.48550/ARXIV.2203.09083. URL <https://arxiv.org/abs/2203.09083>.
- ¹²⁹ Areg Ghazaryan, Tobias Holder, Maksym Serbyn, and Erez Berg. Unconventional superconductivity in systems with annular fermi surfaces: Application to rhombohedral trilayer graphene. *Phys. Rev. Lett.*, 127:247001, Dec 2021. doi: 10.1103/PhysRevLett.127.247001. URL <https://link.aps.org/doi/10.1103/PhysRevLett.127.247001>.
- ¹³⁰ Da-Chuan Lu, Taige Wang, Shubhayu Chatterjee, and Yi-Zhuang You. Correlated metals and unconventional superconductivity in rhombohedral trilayer graphene: A renormalization group analysis. *Phys. Rev. B*, 106:155115, Oct 2022. doi: 10.1103/PhysRevB.106.155115. URL <https://link.aps.org/doi/10.1103/PhysRevB.106.155115>.
- ¹³¹ Huijia Dai, Runyu Ma, Xiao Zhang, and Tianxing Ma. Quantum monte carlo study of superconductivity in rhombohedral trilayer graphene under an electric field. *arXiv*, 2022. doi: 10.48550/ARXIV.2204.06222. URL <https://arxiv.org/abs/2204.06222>.
- ¹³² Huijia Dai, Junchen Hou, Xiao Zhang, Ying Liang, and Tianxing Ma. Mott insulating state and $d + id$ superconductivity in an abc graphene trilayer. *Phys. Rev. B*, 104:035104, Jul 2021. doi: 10.1103/PhysRevB.104.035104. URL <https://link.aps.org/doi/10.1103/PhysRevB.104.035104>.
- ¹³³ The valley and spin degrees of freedom can also be locked in the normal phase, when interactions lead to broken symmetry metallic phases^[146].
- ¹³⁴ W. Kohn and J. M. Luttinger. New mechanism for superconductivity. *Phys. Rev. Lett.*, 15:524–526, Sep 1965. doi: 10.1103/PhysRevLett.15.524. URL <https://link.aps.org/doi/10.1103/PhysRevLett.15.524>.
- ¹³⁵ Saurabh Maiti and Andrei V. Chubukov. Superconductivity from repulsive interaction. In *AIP Conference Proceedings*, volume 1550, page 3, 2013. doi: <https://doi.org/10.1063/1.4818400>.
- ¹³⁶ M. J. Calderón, A. Camjayi, and E. Bascones. Mott correlations in abc graphene trilayer aligned with hbn. *Phys. Rev. B*, 106:L081123, Aug 2022. doi: 10.1103/PhysRevB.106.L081123. URL <https://link.aps.org/doi/10.1103/PhysRevB.106.L081123>.
- ¹³⁷ Chunli Huang, Tobias Wolf, Wei Qin, Nemin Wei, Igor Blinov, and Allan MacDonald. Spin and orbital metallic magnetism in rhombohedral trilayer graphene. *arXiv*, 2022. doi: 10.48550/ARXIV.2203.12723. URL <https://arxiv.org/abs/2203.12723>.
- ¹³⁸ Vladimir Juričić, Enrique Muñoz, and Rodrigo Soto-Garrido. Optical conductivity as a probe of the interaction-driven metal in rhombohedral trilayer graphene. *Nanomaterials*, 12:2927, 2022. doi: <https://doi.org/10.3390/nano12213727>.
- ¹³⁹ Areg Ghazaryan, Tobias Holder, Erez Berg, and Maksym Serbyn. Multilayer graphenes as a platform for interaction-driven physics and topological superconductivity. 2022. doi: 10.48550/arxiv.2211.02492. URL <https://arxiv.org/abs/2211.02492>.

- ¹⁴⁰ Aviram Uri, Sameer Grover, Yuan Cao, John A. Crosse, Kousik Bagani, Daniel Rodan-Legrain, Yuri Myasoedov, Kenji Watanabe, Takashi Taniguchi, Pilkyung Moon, Mikito Koshino, Pablo Jarillo-Herrero, and Eli. Zeldov. Mapping the twist-angle disorder and landau levels in magic-angle graphene. *Nature*, 581(7806):47–52, 2020. doi: <https://doi.org/10.1038/s41586-020-2255-3>.
- ¹⁴¹ Nathanael P Kazmierczak, Madeline Van Winkle, Colin Ophus, Karen C Bustillo, Stephen Carr, Hamish G Brown, Jim Ciston, Takashi Taniguchi, Kenji Watanabe, and D. Kwabena Bediako. Strain fields in twisted bilayer graphene. *Nature Materials*, 20:956, 2021. doi: <https://doi.org/10.1038/s41563-021-00973-w>.
- ¹⁴² Chun Ning Lau, Marc W Bockrath, Kin Fai Mak, and Fan Zhang. Reproducibility in the fabrication and physics of moiré materials. *Nature*, 602(7895):41–50, 2022. doi: <https://doi.org/10.1038/s41586-021-04173-z>.
- ¹⁴³ Yuan Cao, Daniel Rodan-Legrain, Oriol Rubies-Bigorda, Jeong Min Park, Kenji Watanabe, Takashi Taniguchi, and Pablo Jarillo-Herrero. Tunable correlated states and spin-polarized phases in twisted bilayer–bilayer graphene. *Nature*, 583(7815):215–220, jul 2020. ISSN 0028-0836. doi: 10.1038/s41586-020-2260-6. URL <http://arxiv.org/abs/1903.08596><http://dx.doi.org/10.1038/s41586-020-2260-6><http://www.nature.com/articles/s41586-020-2260-6>.
- ¹⁴⁴ Xiaomeng Liu, Zeyu Hao, Eslam Khalaf, Jong Yeon Lee, Yuval Ronen, Hyobin Yoo, Danial Haei Najafabadi, Kenji Watanabe, Takashi Taniguchi, Ashvin Vishwanath, and Philip Kim. Tunable spin-polarized correlated states in twisted double bilayer graphene. *Nature*, 583(7815):221–225, jul 2020. ISSN 0028-0836. doi: 10.1038/s41586-020-2458-7. URL <http://arxiv.org/abs/1903.08130><http://dx.doi.org/10.1038/s41586-020-2458-7><http://www.nature.com/articles/s41586-020-2458-7>.
- ¹⁴⁵ Kin Fai Mak and Jie Shan. Semiconductor moiré materials. *Nature Nanotech.*, 17:686, 2022. doi: <https://doi.org/10.1038/s41565-022-01165-6>.
- ¹⁴⁶ Ethan Lake, Adarsh S. Patri, and T. Senthil. Pairing symmetry of twisted bilayer graphene: A phenomenological synthesis. *Phys. Rev. B*, 106:104506, Sep 2022. doi: 10.1103/PhysRevB.106.104506. URL <https://link.aps.org/doi/10.1103/PhysRevB.106.104506>.